Progress In Electromagnetics Research C, Vol. 125, 201–216, 2022

A Mode Switchable Ferrite Composite Right/Left Handed Microwave Coupler

Mahmoud A. Abdalla[1, *] and Zhirun Hu[2]

Abstract—In this paper, novel mode switchable microwave coupled line couplers on ferrite substrates are presented. The couplers are realized in Composite Right/Left Handed coplanar waveguide configurations. Two different types of mode switchable couplers are proposed. The first one can switch the power from the backward coupling port to the through port. The second one can switch the power from the backward coupling port to both the through and forward coupling ports. In both cases, the mode switching is achieved by varying the applied DC magnetic bias. The theoretical analysis of the switching mechanism has been carried out based on the general coupled mode approach. The analysis is then verified numerically and experimentally. The measurement results confirm the switching functionalities of the fabricated couplers with better than 10 dB isolation between the switched signals. Moreover, these novel mode switchable couplers are compact and require very low external DC magnetic bias due to their CPW configurations. These new proposed switches can be applied in the smart microwave components in different radar/communication application.

1. INTRODUCTION

Over the two pasting decades, there has been renewed scientific research in using structures to develop artificial materials, also known as metamaterials since such materials can provide new functionalities which cannot be achieved otherwise. Left-handed metamaterials (LHMs) are the structures that can demonstrate negative permittivity and permeability together. The realization of LHMs in the form of a Composite Right/Left Handed (CRLH) transmission line (TL) is one of the popular realization structures in which LHM is realized by periodically loading a TL by series capacitors and shunt inductors. CRLH TL has been realized as 1D TL structures in which the propagation is only along the structure principal axis [1–4].

In the literature, different realizations of non-resonant 1-D CRLH TLs in either microstrip [5, 6] or CPW [7–12] have been proposed. Based on these novel transmission lines, several microwave components such as balun, couplers, power dividers, filters, and antennas [13–33] have been developed.

Coplanar waveguide structures are very attractive in microwave engineering. Moreover, the ferrite coplanar waveguide transmission line needs a smaller DC biasing magnetic field as a consequence of its small demagnetization factor concerning microstrip one. Examples of many non-reciprocal CPW couplers, isolators, and circulators are presented in [34–36].

Mixing the features of CRLH TLs and the ferrite substrates in mixed dielectric/ferrite substrate microstrip lines [37, 38] and ferrite substrate CPW lines [39, 40]. Applying these TL configurations, many other reviewers have presented a tunable microwave device such as resonators [41, 42], impedance transformers [43, 44], phase shifters [45, 46], diplexers [47], isolators [48], circulators [49], leaky wave antennas [50–54], and couplers [55–60].

Received 27 September 2022, Accepted 18 October 2022, Scheduled 24 October 2022
* Corresponding author: Mahmoud Abdelrahman Abdalla (maaabdalla@ieee.org).
[1] Electronic Engineering Department, Military Technical College, Cairo, Egypt. [2] AMACG, EEE School, University of Manchester, UK.

For a conventional coupled line coupler (CLC), either backward or forward, its size depends on the operating frequency such that the size is related to the electrical length which is decreased by decreasing the frequency. If the two coupled lines are made of left-handed transmission lines, they can achieve larger electric lengths at lower frequencies. Furthermore, a CRLH CLC can achieve a quasi-zero dB coupling level with an easily realizable gap between two lines [61].

Yet to the moment, and up to the knowledge of the authors, no research is focused on the use of the tunable/non-reciprocal properties of the ferrite CRLH transmission lines to introduce switch devices. The switching can be done through the control of the power flow in ferrite CRLH couplers from the through, backward coupling, and forward coupling ports. Since the basic principles are similar and to prove the generality of the idea, in this paper, we propose two different types of novel mode switchable CRLH ferrite CLCs to illustrate the two different power switching phenomena. The first switch is switching between through and backward coupling ports whereas the second one switches between the backward and forward coupling ports. Both couplers were implemented using CPW configuration over a ferrite substrate. The couplers were discussed in the context of design principles, circuit simulation, EM simulations, and experimental measurements.

Thanks to these power control, the switches can switch power in different directions, so this can be applied in new approach for reconfigurable components in smart wireless systems.

2. THEORY

2.1. Design Guides for CRLH Coupled Line Coupler

By applying the coupled mode theory, the CRLH CLC coupling coefficients for the backward mechanism (C_{BW}) and forward mechanism (C_{FW}) can be calculated as [20]

$$C_{BW} = \beta_R \left(\frac{\kappa_e + \kappa_m}{2}\right) \tag{1}$$

$$C_{FW} = \beta_R \left(\frac{\kappa_m - \kappa_e}{2}\right) \tag{2}$$

where β_R is the propagation constant along the individual hosting right-handed TL whereas κ_e is the electric and coupling coefficient, and κ_m is magnetic [61]

$$\kappa_m = (L_m/L_R) \tag{3}$$

$$\kappa_e = (C_e/C_R) \tag{4}$$

where L_m is the mutual inductance; C_e is the mutual capacitance; and L_R and C_R are the parasitic inductance and capacitance.

The coupling mode can then be decided as follows:

1- A typical backward coupler, i.e., κ_m, is positive and $= \kappa_e$,

$$C_{BW} = (L_m/L_R)\,\beta_R \tag{5}$$

$$C_{FW} = 0 \tag{6}$$

2- A typical forward coupler, i.e., $\kappa_m = -\kappa_e$,

$$C_{BW} = 0 \tag{7}$$

$$C_{FW} = -(L_m/L_R)\,\beta_R \tag{8}$$

A flowchart for the design guides for the CRLH Coupled Line Coupler is shown in Fig. 1(a).

2.2. Design Principles for Ferrite CRLH CLC

It has been explained in [38] that the ferrite TL can demonstrate effective positive/negative magnetic permeability depending on the external DC bias. The negative permeability is equivalent to a negative series inductive load (capacitive load).

Therefore, within the negative ferrite permeability frequency band, L_R is negative. Hence, from (3), the magnetic coupling coefficient, κ_m, alters its sign as permeability does. In other words, for a CLC having a positive κ_m, the CLC is a backward coupler. Should the ferrite permeability alter to be negative within the same frequency band, i.e., κ_m changes its sign to be negative, the CLC becomes a forward coupler. As ferrite permeability changes its sign, the coupling mode of the CLC changes from backward to forward. This can be achieved by the DC magnetic bias which in turn will change the ferrite permeability sign and so the coupling coefficient κ_m.

As a physical explanation, the nonreciprocal properties of ferrite substrate when the permeability is negative do not allow the backward mode propagations. Instead, they enhance any forward mode propagations. As a result, using a proper DC magnetic bias, the CRLH CLC outputs can be switched from backward to through or through/forward ports and vise versa as will be illustrated later. A flowchart for the design guides for the Ferrite CRLH coupled line coupler is shown in Fig. 1(b).

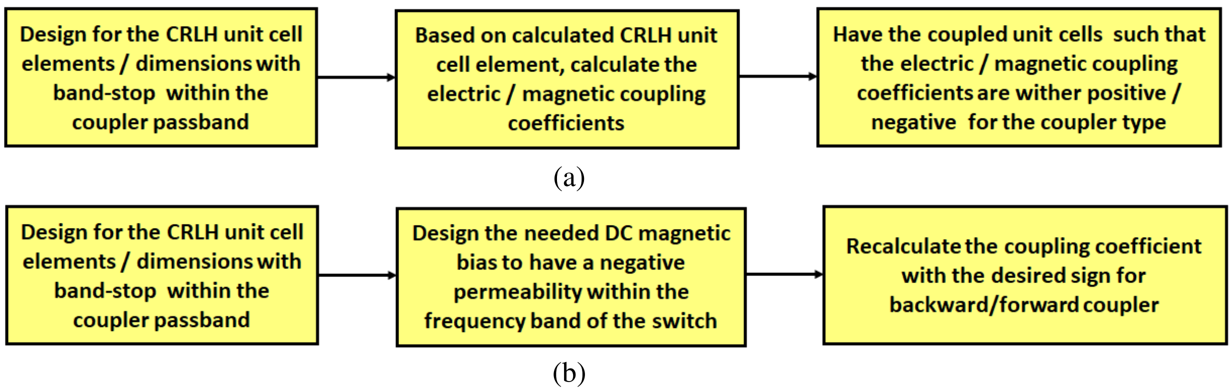

Figure 1. A flowchart for the design guides for (a) CRLH coupled line coupler, (b) ferrite CRLH CLC.

2.3. Ferrite Coupled Line Coupler

The front cross-section of the presented CLCs in this work is shown in Fig. 2. The used ferrite substrate is YIG Trans Tech TTVG-1850 with $\varepsilon_f = 14.8 \pm 5\%$, $\tan\delta < 0.0002$, $4\pi M_S = 1850 \pm 5\%$ Gauss, $\Delta H_0 \leq 10$ Oe. The DC internal magnetic field (H_0) direction is shown such that the ferrite permeability tensor $[\mu]$ is then calculated as [62]

$$[\mu] = \mu_0 \begin{bmatrix} 1 & 0 & 0 \\ 0 & \mu_f & jk \\ 0 & -jk & \mu_f \end{bmatrix} \tag{9}$$

where

$$\mu_f = \frac{\omega_{hm}^2 - \omega^2}{\omega_h^2 - \omega^2} \tag{10}$$

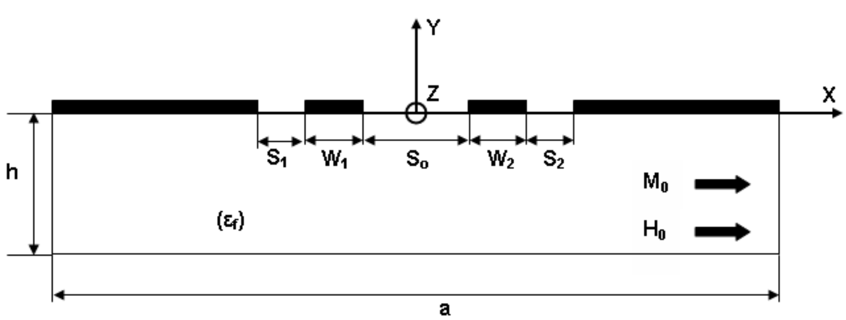

Figure 2. The front cross section of the different ferrite CRLH CPW CLC Switch.

$$k = \frac{\omega\omega_m}{\omega_h^2 - \omega^2} \tag{11}$$

$$\omega_h = \mu_0\gamma H_0, \quad \omega_{hm} = \mu_0\gamma\sqrt{H_0(H_0 + M_S)}, \quad \omega_m = \mu_0\gamma M_S \tag{12}$$

where γ is the gyromagnetic ratio of the ferrite, and μ_0 is the free space permeability.

3. BACKWARD/THROUGH COUPLING (BC/T) CRLH CPW CLC SWITCH

3.1. Backward/Through Switch Design Procedures

The ferrite (BC/T) CRLH CPW CLC Switch layout is shown in Fig. 3(a). The coupler switches its output from the backward output to nonreciprocal through output.

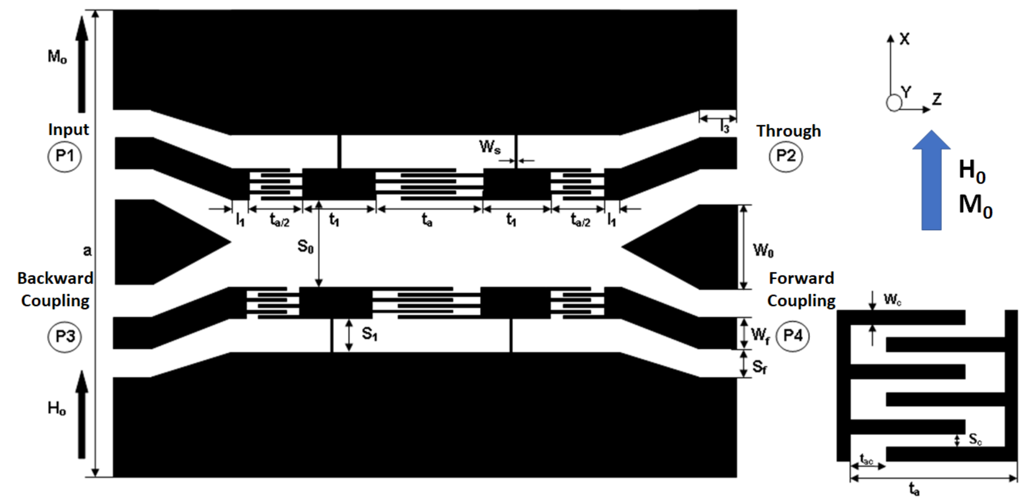

(a) (b)

Figure 3. (a) The layout geometry of the ferrite (BC/T) CRLH CPW CLC Switch, $a = 19.8$ mm, $L = 10.2$ mm, $W_0 = 6$ mm, $t_a = 2.0$ mm, $t_1 = 1.5$ mm, $l_1 = 0.25$ mm, $S_o = 0.5$ mm, $S_f = 0.8$ mm, $W_f = 1.3$ mm, $W_s = 0.25$ mm, and $l_3 = 0.1$ mm. (b) The inter digital capacitor geometry $S_c = W_c = 0.1$ mm and $t_{ac} = 0.2$ mm.

The coupler is designed using two individual identical coupled CRLH TLs realized using a CPW TL loaded periodically with a CRLH unit cell composed of a shunt strip inductor and series interdigital capacitor as plotted in Fig. 3(b). For a proper matching, different capacitor dimensions were used. The coupler was ended by four 50 Ω CPW terminals. The equivalent circuit of the coupler is shown in Fig. 4.

The design procedures of the backward/through switchable ferrite CRLH CPW CLC were fulfilled in the following steps. The first step is to design a backward CLC with high backward coupling, close to 0 dB. This step can be achieved using the general principles of arbitrary coupling levels of conventional CRLH backward CLCs [61]. The equivalent circuit model design was optimized. Next, the physical layout of the ferrite CRLH CPW CLC was designed. The loading elements, whose values were obtained from the circuit simulations, were calculated analytically as a start. The interdigital capacitors were calculated referring to [3], the inductors to [62], and the CPW parasitic elements to [63, 64].

The initial layout was then optimized using HFSS such that it is equivalent to the circuit simulation (in this step, the applied DC magnetic bias was set to a very high value (for $H_0 = 50,000$ Oe)). The final design step was to demonstrate the switching between the backward coupling and a nonreciprocal through port through further optimization of the CLC obtained in the second step for $H_0 = 0$ and a specific DC magnetic bias.

The choice of $H_0 = 0$ Oe was to ensure that the hosting ferrite CPW TL has positive ferrite permeability which can be analytically seen from (10). Thus, this case is practically close to the

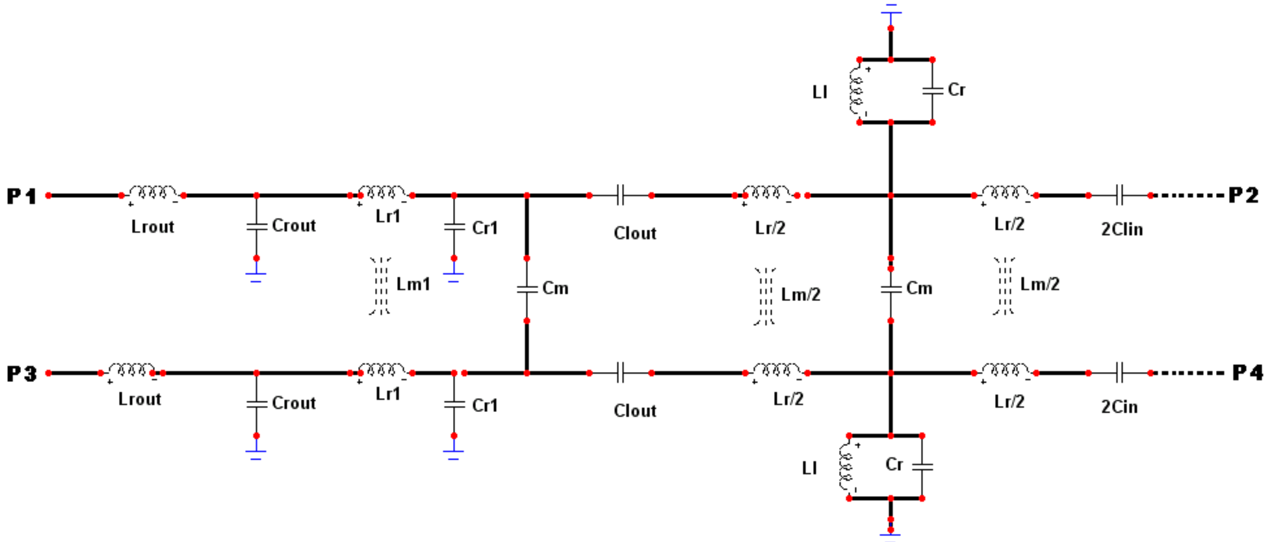

Figure 4. The equivalent circuit model of the ferrite (BC/T) CRLH CPW CLC Switch.

isotropic case at a very high DC magnetic bias. Since the switching frequency band is associated with the negative ferrite permeability bandwidth, the specific DC magnetic bias was selected so that it introduced negative ferrite permeability within the same frequency band having backward coupling for $H_0 = 0$ Oe. In other words, the optimization process was done to achieve two goals: (1), the ferrite CRLH CPW CLC demonstrates a backward coupling for $H_0 = 0$ Oe and (2) a nonreciprocal propagation for other specific H_0 values within the same frequency band. Therefore, the optimization process results in switching between backward coupling and nonreciprocal through ports.

3.2. Simulation Results

In Fig. 5, both circuit and HFSS simulation ($H_0 = 50,000$ Oe) results are good and agree with each other. From 6 GHz to 8 GHz, the coupler backward coupling (S_{31}) is very close to 0 dB; the coupler reflection coefficient (S_{11}) is less than 10 dB; the insertion loss (S_{21}) is lower than 12 dB; and the forward coupling isolation (S_{41}) is less than −20 dB.

Next, the coupler structure was optimized for switching purposes to switch between a backward coupling at $H_0 = 0$ Oe to a nonreciprocal through propagation at $H_0 = 2000$ Oe. The final circuit dimensions were decided as shown in Fig. 3. The HFSS simulated scattering parameters of the coupler at $H_0 = 0$ Oe are shown in Fig. 6. It can be seen that the coupler clearly illustrates backward coupling from 6 GHz to 8 GHz. The average backward coupling (S_{31}) is −1.5 dB, whereas the through (S_{21}) is below −10 dB over most of the band. The highest forward coupling S_{41} is −14 dB at 8 GHz.

The CLC HFSS simulated scattering parameters at $H_0 = 2000$ Oe are plotted in Fig. 7. The through (S_{21}) has become dominant, and backward coupling (S_{31}) has been dramatically reduced. For instance, (S_{21}) is increased from −13 dB (in Fig. 6) to −5 dB, and (S_{31}) is reduced from −2 dB (in Fig. 6) to be less than −30 dB at 7 GHz. Furthermore, the through propagation now becomes nonreciprocal. The highest forward coupling S_{41} is −12 dB at 6 GHz. Based on results in Fig. 6 and Fig. 7 the backward coupling at $H_0 = 0$ Oe is now switched to a nonreciprocal through propagation at $H_0 = 2000$ Oe from 6.2 GHz to 8 GHz.

The frequency band of the negative ferrite permeability for $H_0 = 2000$ Oe can be calculated, approximately, using (10) to be from 5.7 GHz to 7.7 GHz. This reveals that the mechanism of the mode switching is due to the change of permeability from positive to negative. It can also be seen that the switching frequency band illustrated by the simulation results is very close to the analytically calculated bandwidth. The variation between those two bandwidths is due to the simplified definition of ferrite permeability. However, the calculated values can be used as a design guideline.

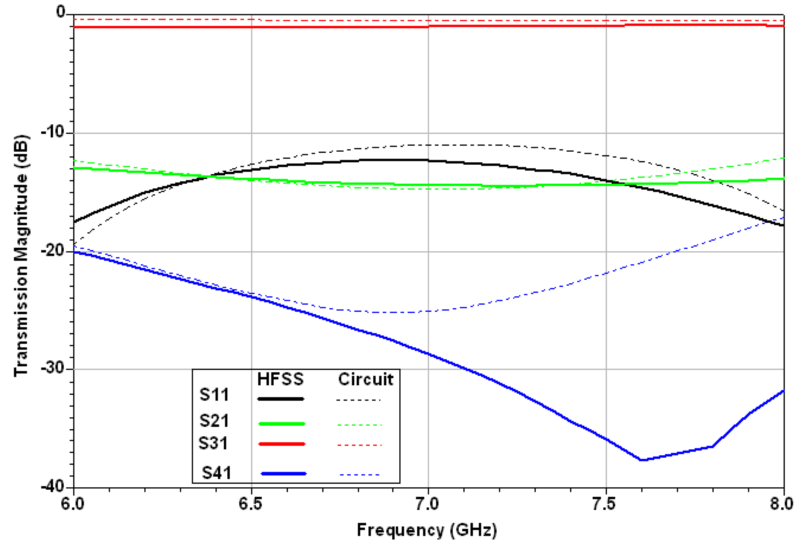

Figure 5. The HFSS and equivalent circuit model simulated S parameter magnitudes of the ferrite (BC/T) CRLH CPW CLC Switch at, $H_0 = 50,000\,\mathrm{Oe}$. Solid lines are for HFSS results and dotted lines for circuit model. $C_{Lout} = 1.6\,\mathrm{pF}$, $C_{Lin} = 1.2\,\mathrm{pF}$, $L_L = 0.45\,\mathrm{nH}$, $K_m = 0.5$, $C_e = 1.4\,\mathrm{pF}$, $C_r = 0.4\,\mathrm{pF}$, $C_{r1} = 0.1\,\mathrm{pF}$, $C_{rout} = 0.4\,\mathrm{pF}$, $L_r = 0.7\,\mathrm{nH}$, $L_{r1} = 0.4\,\mathrm{nH}$, and $L_{rout} = 0.25\,\mathrm{nH}$, $t_1 = 1.1\,\mathrm{mm}$, $t_a = 1.8\,\mathrm{mm}$, and $L = 9\,\mathrm{mm}$.

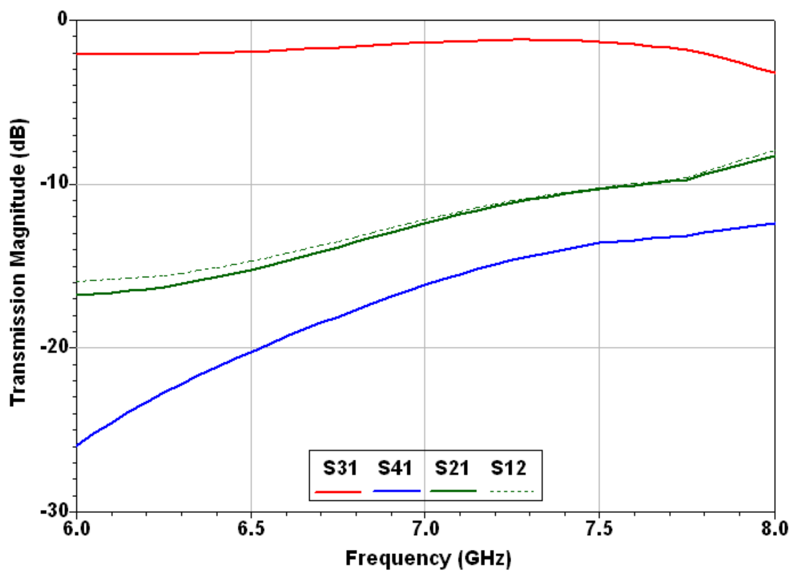

Figure 6. The HFSS simulated S parameter magnitudes of the ferrite (BC/T) CRLH CPW CLC Switch at $H = 0\,\mathrm{Oe}$.

3.3. Fabrication and Experimental Results

The circuit fabrication was done using lithographic technology. The used YIG ferrite material is a one-sided surface — 0.0003 to 0.0005 inch — silver metallization. The fabricated switchable coupler with the size of $19\,\mathrm{mm} \times 13\,\mathrm{mm} \times 1\,\mathrm{mm}$ is shown in Fig. 8(a) and Fig. 8(b) with extra two FR4 supporters (0.6 mm below and 1.5 mm above the coupler) to strengthen the coupler during measurement. The metallization on the FR4 was removed apart from the edges which were connected to the SMA bases. The coupler with 4 SMAs and a lower FR4 cover is depicted in Fig. 8(b).

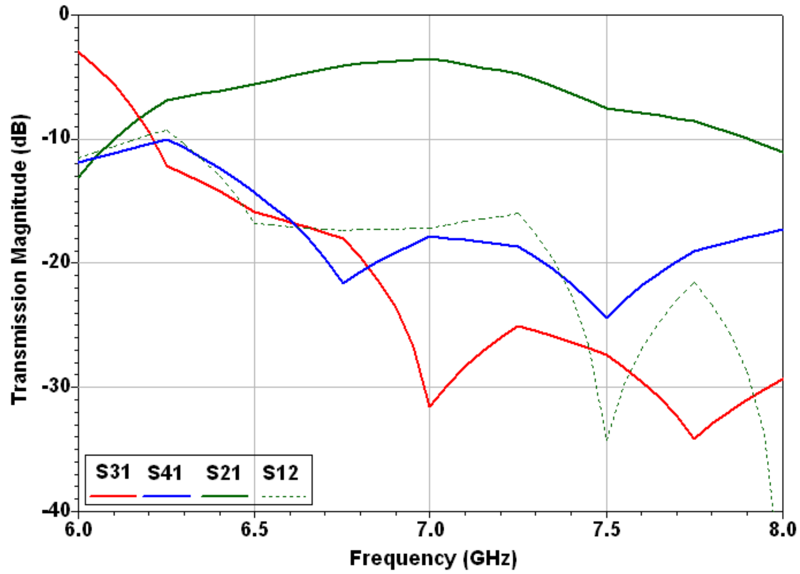

Figure 7. The HFSS simulated S parameters of the ferrite (BC/T) CRLH CPW CLC Switch at $H = 2000\,\mathrm{Oe}$.

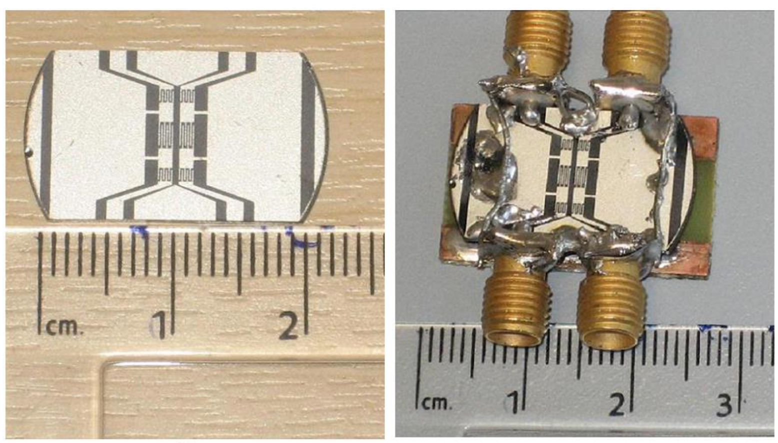

(a) (b)

Figure 8. The TTVG-1850 the ferrite (BC/T) CRLH CPW CLC Switch. (a) The circuit prototype. (b) The lower sided covered circuit prototype.

The measurement setup is shown in Fig. 9 where the coupler was subjected to an external DC magnetic bias generated from an electromagnet. Adjustment of the DC bias direction was specified by the orientation of the coupler between the electromagnet poles. The check of the DC magnetic bias was measured using a Gauss meter, and the scattering parameters magnitude was measured using a VNA.

The external applied DC magnetic bias (H_{ex}) was calculated to compensate for the small effect of the in-plane demagnetization field for more accurate results as

$$H_{ex} = H_0 + 4\pi M_S N \tag{13}$$

where N is the demagnetization factor which was calculated to be approximately 0.05 [65]. From (13), approximately a 90 Oe increase in the external bias field value was applied to compensate for the in-plane demagnetization field.

The scattering parameters of the backward/through switch were measured as in the following paragraphs. In Fig. 10, at $H_0 = 0\,\mathrm{Oe}$, the backward coupling signal is the dominant one. The level

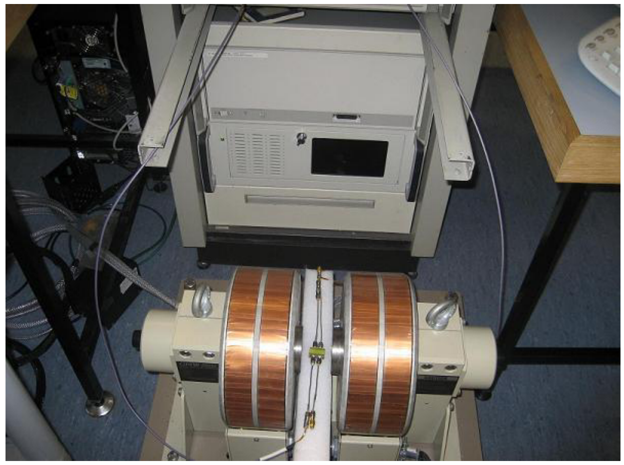

Figure 9. The experimental measurements setting for the *ferrite (BC/T) CRLH CPW CLC Switch measurements.*

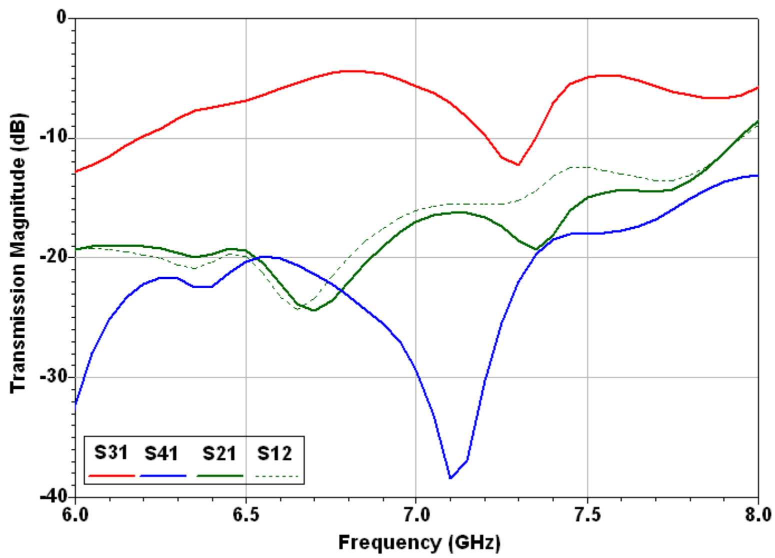

Figure 10. The measured S parameters of the ferrite (BC/T) CRLH CPW CLC Switch at $H = 0\,\mathrm{Oe}$.

of that signal increases from a little below $-10\,\mathrm{dB}$ to reach approximately $-5\,\mathrm{dB}$ in the best cases. On the other hand, the through (S_{21}) and forward coupling (S_{41}) coefficients are around $-20\,\mathrm{dB}$ from 6 GHz to 7 GHz. So, the average backward coupling is 10 dB higher than the through from 6 GHz to 7.5 GHz. In Fig. 11, at $H_0 = 2000\,\mathrm{Oe}$, the dominant output appears at the through port; its level is above $-10\,\mathrm{dB}$ from 6 GHz to 7.5 GHz beyond which it becomes slightly below $-10\,\mathrm{dB}$. On the other hand, the backward coupled signal S_{31} decreases from $-10\,\mathrm{dB}$ at 6 GHz to approximately $-15\,\mathrm{dB}$ at 6.5 GHz, and it becomes less than $-20\,\mathrm{dB}$ from 6.8 GHz and is reduced to below $-24\,\mathrm{dB}$ above 7.5 GHz.

By comparing these levels to their responses at $H_0 = 0\,\mathrm{Oe}$ shown in Fig. 10, we can see that the switching between the backward coupling at $H_0 = 0\,\mathrm{Oe}$ and the through output at $H_0 = 2000\,\mathrm{Oe}$ from 6 GHz to 8 GHz has been realized and experimentally verified. From 6.7 GHz to 7.4 GHz, the backward coupling (S_{31}) and the through (S_{21}) are better than $-9\,\mathrm{dB}$ on average. The through propagation at $H_0 = 2000\,\mathrm{Oe}$ is nonreciprocal.

In summary, the proposed switch based coupler can act as a novel microwave switch between the backward coupling and the through from 6.7 GHz to 7.4 GHz by simply changing H_0 from 0 Oe to 2000 Oe.

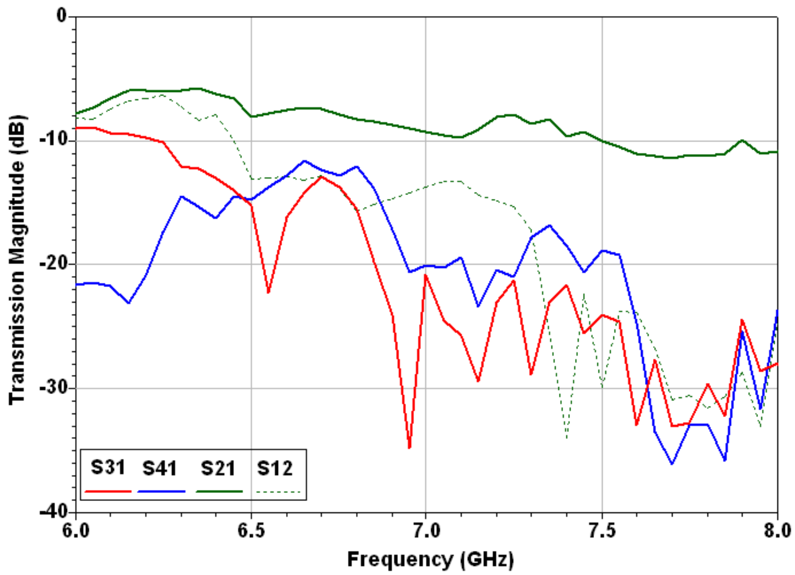

Figure 11. The measured S parameters of ferrite (BC/T) CRLH CPW CLC Switch showing its switching property for $H = 2000$ Oe.

4. BACKWARD/FORWARD-THROUGH (BC/FC-T) CRLH CPW CLC SWITCH

4.1. Layout and Design

The layout of the (BC/FC-T) CRLH CPW CLC Switch is shown in Fig. 12. The coupler switches its output from the backward output to a forward coupling and a nonreciprocal through output. The coupler is designed using two individual identical coupled CRLH TLs realized using a CPW TL loaded periodically with a shunt planar segment inductor and series air gap capacitor. The coupler is ended with four 50 Ω CPW terminals. The coupler was designed and optimized to switch from backward to forward coupling and vice versa by changing H_0 from 0 Oe to 2000 Oe. First, a CRLH backward CLC

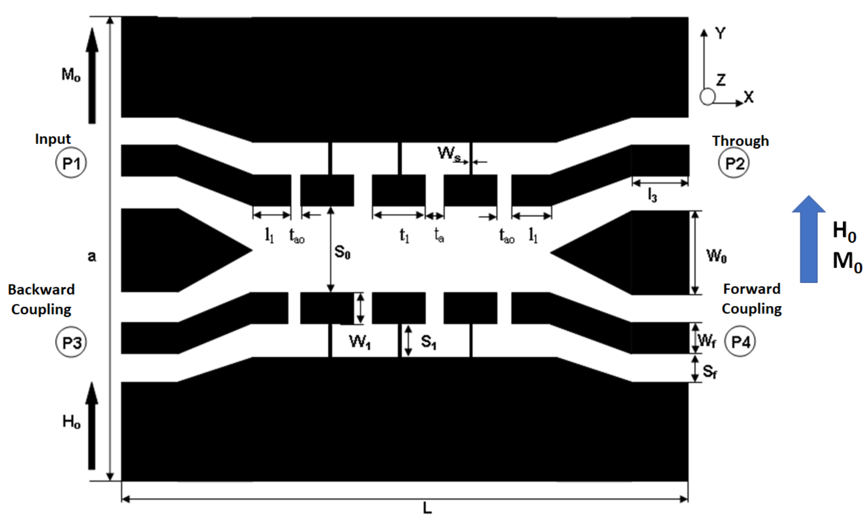

Figure 12. The layout geometry of the ferrite (BC/FC-T) CRLH CPW CLC switch $a = 19.8$ mm, $L = 10.5$ mm, $W_0 = 6$ mm, $t_a = 0.2$ mm, $t_{a0} = 0.25$ mm, $t_1 = 0.5$ mm, $l_1 = 0.1$ mm, $l_3 = 2$ mm, $W_1 = 0.9$ mm, $S_1 = 1.6$ mm, $S_0 = 0.3$ mm, $W_s = 0.1$ mm, $S_f = 0.8$ mm, and $W_f = 1.3$ mm.

within a specific frequency band at $H_0 = 0$ Oe is designed. Within this specific band, the CLC has a positive magnetic coupling coefficient (κ_m). By careful design, this specific frequency band can coincide with the frequency band where the ferrite has negative permeability under a certain DC magnetic bias, $H_0 = 2000$ Oe. Under such DC magnetic bias, the magnetic coupling coefficient, κ_m, becomes negative, meaning that the coupling is no longer backward but forward, i.e., the coupling mode is switched from backward to forward.

4.2. Simulation Results

The full wave simulated scattering parameters of the switch at $H_0 = 0$ Oe are shown in Fig. 13. It can be seen that under this bias the coupler exhibits a dominant backward coupling propagation from 7 GHz up to 8 GHz. The backward coupling level is approximately -10 dB over this band. The forward coupling level is approximately below -20 dB whereas the through level is around -30 dB.

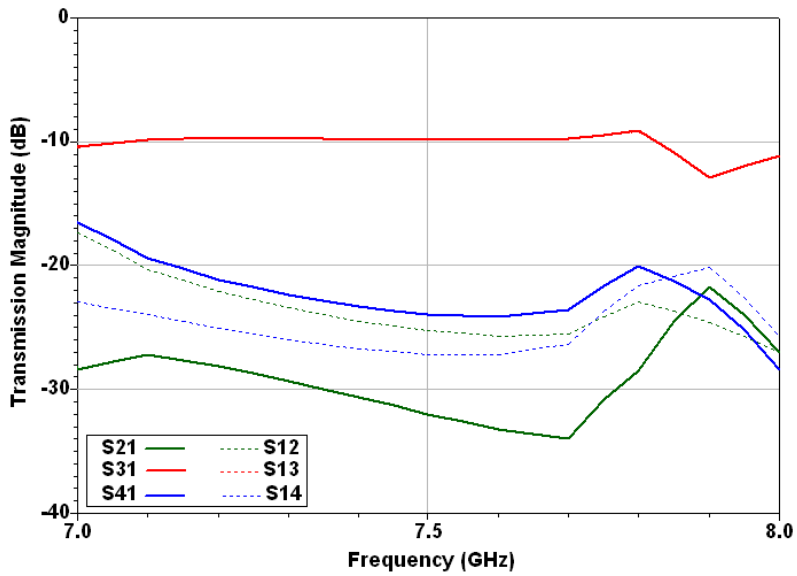

Figure 13. The HFSS simulated S parameters of the ferrite (BC/FC-T) CRLH CPW CLC Switch at $H = 0$ Oe.

The simulated scattering magnitudes of the coupler at $H_0 = 2000$ Oe are shown in Fig. 14, illustrating that backward coupling has now been reduced significantly, whereas the forward and through have been increased dramatically. For instance, at 7.3 GHz the backward coupling is around -30 dB, and forward and through are around -8 dB and -12 dB, respectively, clearly demonstrating that the coupling mode has been switched from backward to forward/through as H_0 changes from 0 Oe to 2000 Oe. Also, both the through and forward coupling signals have nonreciprocal properties.

4.3. Experimental Results

The measurement setup and procedures were the same as explained in Section 3.4. The fabricated coupler has a size of 19.8 mm $\times$ 10.5 mm $\times$ 1 mm as shown in Fig. 15(a). The coupler was supported with two horizontal FR4 PCB covers of 1.5 mm thickness soldered to the SMAs connectors at both ends, shown in Fig. 15(b). During measurements, approximately an extra 90 Oe was applied to compensate for the demagnetization field. The measured scattering parameters of the coupler at $H_0 = 0$ Oe and $H_0 = 2000$ Oe from 7 GHz to 8 GHz are shown in Fig. 16 and Fig. 17, respectively. In Fig. 16, at $H_0 = 0$ Oe, it can be seen that the coupler has dominant backward coupling output. For instance, at 7.3 GHz, the backward coupling level is about -11 dB, which is more than 10 dB higher than the

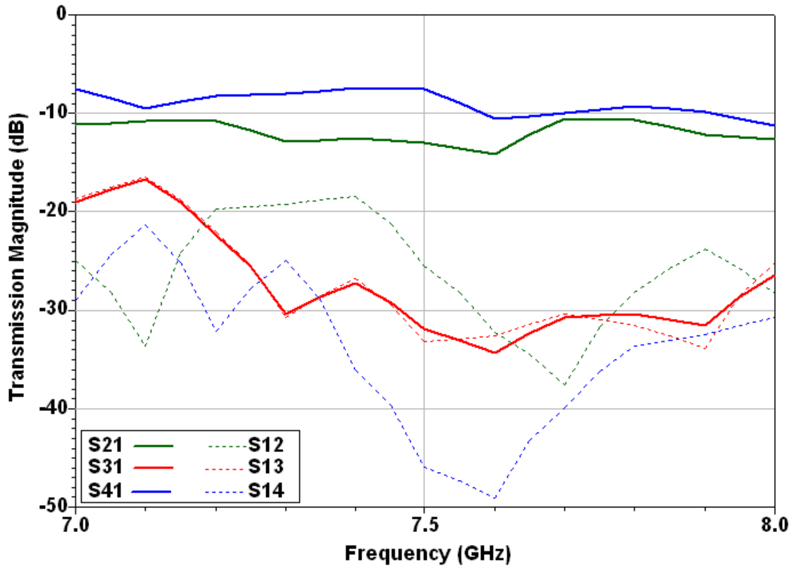

Figure 14. The HFSS simulated S parameters of the ferrite (BC/FC-T) CRLH CPW CLC Switch at $H = 2000\,\mathrm{Oe}$.

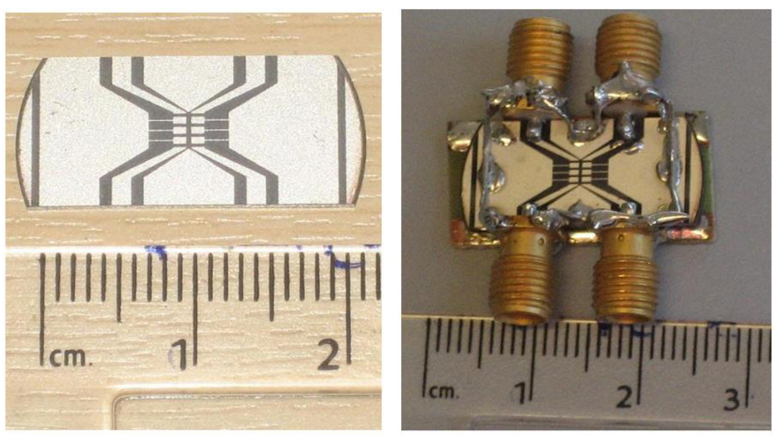

(a) (b)

Figure 15. The ferrite (BC/FC-T) CRLH CPW CLC switch. (a) The circuit prototype. (b) The lower sided covered circuit prototype.

through and 20 dB higher than the forward coupling. Higher than 7.4 GHz, the differences between the backward and forward/through decrease, but the backward coupling still dominates up to 7.9 GHz.

In Fig. 17, at $H_0 = 2000\,\mathrm{Oe}$, both the forward coupling and the through signals have increased. For instance, at 7.3 GHz the forward coupling is now about -12 dB, and so is the through, whereas the backward coupling has reduced to -24 dB. More detailed comparisons between Figs. 16 and 17 reveal that from 7.2 GHz to 7.4 GHz, the forward coupling S_{41} gains at least a 15 dB increase, from around -30 dB at $H_0 = 0$ to approximately -12 dB at $H_0 = 2000$, and the through has an approximately 10 dB increase, from around -22 dB at $H_0 = 0$ to approximately -12 dB at $H_0 = 2000$. On the other hand, the backward coupling S_{31} decreases from approximately -12 dB at $H_0 = 0\,\mathrm{Oe}$ to less than -25 dB at $H_0 = 2000\,\mathrm{Oe}$ over the same frequency band. The backward mode has been switched to forward/through modes as magnetic bias alters from 0 Oe to 2000 Oe, hence experimentally verifying our theoretical prediction and numerical simulation results. It is also noticed that both through and

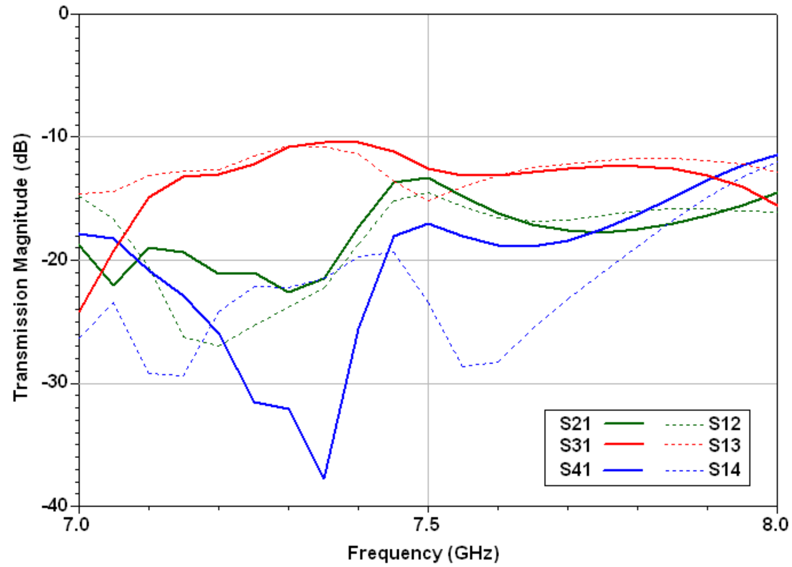

Figure 16. The measured S parameters magnitudes of the ferrite (BC/FC-T) CRLH CPW CLC Switch at $H = 0\,\mathrm{Oe}$.

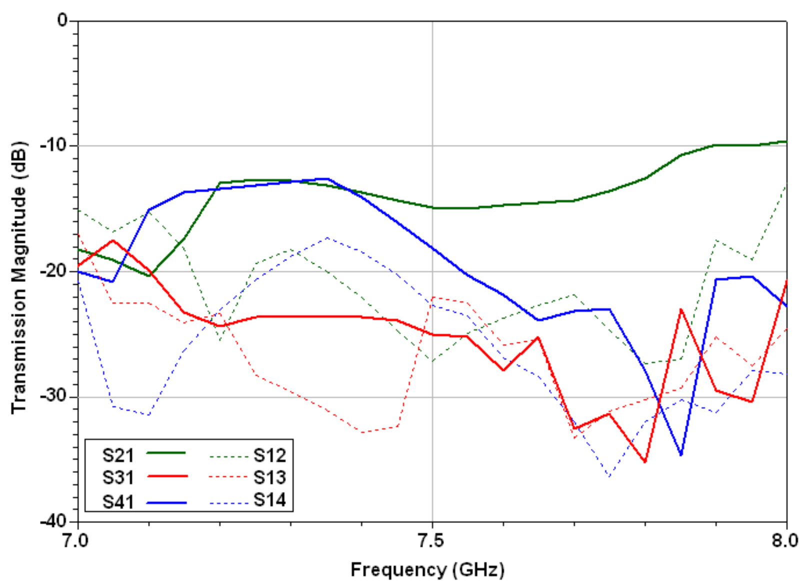

Figure 17. The measured S parameters magnitudes of the ferrite (BC/FC-T) CRLH CPW CLC Switch at $H = 2000\,\mathrm{Oe}$.

forward coupling have nonreciprocal properties.

It is obvious, from Fig. 14 to Fig. 17, that the measured bandwidth of the mode switchable CLC is much narrower than that of HFSS simulation results. The exact cause of this is not clear. However, this discrepancy should not detract from the message being conveyed — experimental verification of the mode switchable CRLH CLC.

As an advantage, the backward mode in the coupler is switched to forward and through modes as magnetic bias alters from 0 Oe to 2000 Oe. These are the double advantages of the first proposed coupler.

5. CONCLUSION

Two novel ferrite microwave power switching devices have been presented. These devices have been designed and realized as ferrite CRLH CLCs in CPW configurations. The novel CLCs demonstrate new functionalities — mode switchable, i.e., the CLCs can switch the power between the backward and through ports, or between the backward and forward/through ports as magnetic bias changes with nonreciprocity. The theoretical concepts of the switching mechanism have been discussed and validated using full-wave electromagnetic numerical simulations. CLCs based on the full-wave simulation results were fabricated, and the mode switchable functionalities have been experimentally verified. Moreover, the reported CLCs are compact and have a low demagnetization factor. As an advantage of the proposed switch, it can be claimed that this new mode switchable CLCs can find their applications in smat/reconfigurable radar systems and cognitive radio communications.

REFERENCES

1. Eleftheriades, G. V., A. K. Iyer, and P. C. Kremer, "Planar negative refractive index media using periodically L-C loaded transmission lines," *IEEE Transactions on Microwave Theory and Techniques*, Vol. 50, 2702–2712, 2002.
2. Caloz, C. and T. Itoh, "Transmission line approach of left-handed (LH) materials and microstrip implementation of an artificial LH transmission line," *IEEE Transactions on Antennas and Propagation*, Vol. 52, 1159–1166, 2004.
3. Caloz, C. and T. Itoh, *Electromagnetic Metamaterials Transmission Line Theory and Microwave Applications*, John Wiey & Sons, New Jersey, 2006.
4. Caloz, C., "Metamaterial dispersion engineering concepts and applications," *Proceedings of the IEEE*, Vol. 99, No. 10, 1711–1719, 2011.
5. Liu, C. and W. Menzel, "Broadband via-free microstrip balun using metamaterial transmission lines," *IEEE Microwave and Wireless Components Letters*, Vol. 18, No. 7, 437–439, 2008.
6. Sarkar, A., D. A. Pham, and S. Lim, "Tunable higher order mode-based dual-beam CRLH microstrip leaky-wave antenna for V-band backward-broadside-forward radiation coverage," *IEEE Transactions on Antennas and Propagation*, Vol. 68, No. 10, 6912–6922, 2020.
7. Mao, S.-G., M.-S. Wu, Y.-Z. Chueh, and C. H. Chen, "Modeling of symmetric composite right/left-handed coplanar waveguides with applications to compact bandpass filters," *IEEE Transactions on Microwave Theory and Techniques*, Vol. 53, 3460–3466, 2005.
8. Gao, J. and L. Zhu, "Characterization of infinite- and finite-extent coplanar waveguide metamaterials with varied left- and right-handed passbands," *IEEE Microwave and Wireless Components Letters*, Vol. 15, 805–807, 2005.
9. Chiu, S.-C., C.-P. Lai, and S.-Y. Chen, "Compact CRLH CPW antennas using novel termination circuits for dual-band operation at zeroth-order series and shunt resonances," *IEEE Transactions on Antennas and Propagation*, Vol. 61, No. 3, 1071–1080, 2012.
10. Chi, P.-L. and Y.-S. Shih, "Compact and bandwidth-enhanced zeroth-order resonant antenna," *IEEE Antennas and Wireless Propagation Letters*, Vol. 14, 285–288, 2014.
11. Elsheikh, M. A. G., N. Y. Ammar, and A. M. E. Safwat, "Analysis and design guidelines for wideband CRLH SRR-loaded coplanar waveguide," *IEEE Transactions on Microwave Theory and Techniques*, Vol. 68, No. 7, 2562–2570, 2020.
12. El Atrash, M., M. A. Abdalla, and H. M. Elhennawy, "A compact highly efficient Π-section CRLH antenna loaded with textile AMC for wireless body area network applications," *IEEE Transactions on Antennas and Propagation*, Vol. 69, No. 2, 648–657, Feb. 2021.
13. Vélez, P., M. Durán-Sindreu, A. Fernández-Prieto, J. Bonache, F. Medina, and F. Martı, "Compact dual-band differential power splitter with common-mode suppression and filtering capability based on differential-mode composite right/left-handed transmission-line metamaterials," *IEEE Antennas and Wireless Propagation Letters*, Vol. 13, 536–539, 2014.

14. Liu, F.-X. and J.-C. Lee, "A dual-mode power divider with embedded meta-materials and additional grounded resistors," *IEEE Transactions on Microwave Theory and Techniques*, Vol. 69, No. 8, 3607–3615, 2021.
15. Huang, T., L. Feng, L. Geng, H. Liu, S. Y. Zheng, S. Ye, L. Zhang, and H. Xu, "Compact dual-band Wilkinson power divider design using via-free D-CRLH resonators for Beidou navigation satellite system," *IEEE Transactions on Circuits and Systems II: Express Briefs*, Vol. 69, No. 1, 65–69, 2021.
16. Liu, F.-X., Y. Wang, S.-P. Zhang, and J.-C. Lee, "Design of compact tri-band Gysel power divider with zero-degree composite right-/left-hand transmission lines," *IEEE Access*, Vol. 7, 34964–34972, 2019.
17. Ren, X., K. Song, M. Fan, Y. Zhu, and B. Hu, "Compact dual-band Gysel power divider based on composite right-and left-handed transmission lines," *IEEE Microwave and Wireless Components Letters*, Vol. 25, No. 2, 82–84, 2014.
18. Chi, P.-L. and T.-Y. Chen, "Dual-band ring coupler based on the composite right/left-handed folded substrate-integrated waveguide," *IEEE Microwave and Wireless Components Letters*, Vol. 24, No. 5, 330–332, 2014.
19. Chang, L. and T.-G. Ma, "Dual-mode branch-line/rat-race coupler using composite right-/left-handed lines," *IEEE Microwave and Wireless Components Letters*, Vol. 27, No. 5, 449–451, 2017.
20. Abdalla, M. A., M. A. Fouad, H. A. Elregeily, and A. A. Mitkees, "Wideband negative permittivity metamaterial for size reduction of stopband filter in antenna applications," *Progress In Electromagnetics Research C*, Vol. 25, 55–66, 2011.
21. Mohan, M. P., A. Alphones, and M. F. Karim, "Triple band filter based on double periodic CRLH resonator," *IEEE Microwave and Wireless Components Letters*, Vol. 28, No. 3, 212–214, 2018.
22. Song, Y., P. Wen, H. Liu, Y. Wang, and L. Geng, "Design of compact balanced-to-balanced diplexer using dual-mode CRLH resonator for RFID and 5G applications," *IEEE Journal of Radio Frequency Identification*, Vol. 3, No. 3, 143–148, 2019.
23. Song, Y., H. Liu, W. Zhao, P. Wen, and Z. Wang, "Compact balanced dual-band bandpass filter with high common-mode suppression using planar via-free CRLH resonator," *IEEE Microwave and Wireless Components Letters*, Vol. 28, No. 11, 996–998, 2018.
24. Shen, G., W. Che, Q. Xue, and W. Yang, "Characteristics of dual composite right/left-handed unit cell and its applications to bandpass filter design," *IEEE Transactions on Circuits and Systems II: Express Briefs*, Vol. 65, No. 6, 719–723, 2017.
25. Shen, G., W. Che, Q. Xue, and W. Feng, "Novel design of miniaturized filtering power dividers using dual-composite right-/left-handed resonators," *IEEE Transactions on Microwave Theory and Techniques*, Vol. 66, No. 12, 5260–5271, 2018.
26. Guan, X., H. Su, H. Liu, P. Wen, W. Liu, P. Gui, and B. Ren, "Miniaturized high temperature superconducting bandpass filter based on D-CRLH resonators," *IEEE Transactions on Applied Superconductivity*, Vol. 29, No. 5, 1–4, 2019.
27. Wang, Z., Y. Ning, and Y. Dong, "Hybrid metamaterial-TL based, low-profile, dual-polarized omnidirectional antenna for 5G indoor application," *IEEE Transactions on Antennas and Propagation*, Vol. 70, No. 4, 2561–2570, 2021.
28. Wang, Z., T. Liang, and Y. Dong, "Composite right-/left-handed-based, compact, low-profile, and multifunctional antennas for 5G applications," *IEEE Transactions on Antennas and Propagation*, Vol. 69, No. 10, 6302–6311, 2021.
29. Huang, T., L. Feng, L. Geng, H. Liu, S. Y. Zheng, S. Ye, L. Zhang, and H. Xu, "Compact dual-band Wilkinson power divider design using via-free D-CRLH resonators for Beidou navigation satellite system," *IEEE Transactions on Circuits and Systems II: Express Briefs*, Vol. 69, No. 1, 65–69, 2021.
30. Sun, Q., Y.-L. Ban, Y.-X. Che, and Z. Nie, "Coexistence-mode CRLH SIW transmission line and its application for longitudinal miniaturized butler matrix and multibeam array antenna," *IEEE Transactions on Antennas and Propagation*, Vol. 69, No. 11, 7593–7603, 2021.

31. Wang, Z., Y. Dong, and T. Itoh, "Miniaturized wideband CP antenna based on metaresonator and CRLH-TLs for 5G new radio applications," *IEEE Transactions on Antennas and Propagation*, Vol. 69, No. 1, 74–83, 2020.
32. Xu, H.-X., G.-M. Wang, X. Chen, and T.-P. Li, "Broadband balun using fully artificial fractal-shaped composite right/left handed transmission line," *IEEE Microwave and Wireless Components Letters*, Vol. 22, No. 1, 16–18, 2012.
33. Xu, H.-X., G.-M. Wang, M.-Q. Qi, C.-X. Zhang, J.-G. Liang, J.-Q. Gong, and Y.-C. Zhou, "Analysis and design of two-dimensional resonant-type composite right left handed transmission lines with compact gain-enhanced resonant antennas," *IEEE Transactions on Antennas and Propagation*, Vol. 61, No. 2, 735–747, 2013.
34. Koshiji, K. and E. Shu, "Circulators using coplanar waveguide," *Electronics Letters*, Vol. 22, No. 19, 1000–1002, 1986.
35. Bayard, B., D. Vincent, C. R. Simovski, and G. Noyel, "Electromagnetic study of a ferrite coplanar isolator suitable for integration," *IEEE Transactions on Microwave Theory and Techniques*, Vol. 51, No. 7, 1809–1814, 2003.
36. Joseph, S., R. Lebourgeois, Y. Huang, L. Roussel, and A. Schuchinsky, "Low-loss hexaferrite self-biased microstrip and CPW circulators," *Proc. in IEEE 2019 13rd Int. Congress on Artificial Materials for Novel Wave Phenomena (Metamaterials)*, X-372, 2019.
37. Ueda, T. and M. Tsutsumi, "Nonreciprocal left-handed transmission characteristics of microstrip lines on ferrite substrate," *IET Microwaves, Antennas & Propagation*, Vol. 1, 349–354, 2007.
38. Ueda, T. and M. Tsutsumi, "Left-handed transmission characteristics of ferrite microstrip lines without series capacitive loading," *IEICE Transactions on Electronics*, Vol. E89-C, 1318–1323, 2006.
39. Abdalla, M. A. and Z. Hu, "On the study of CWP dual band left handed propagation with reciprocal and nonreciprocal characteristics over ferrite substrates," *2007 IEEE Antennas and Propagation Society International Symposium*, 2578–2581, IEEE, 2007.
40. Abdalla, M. A. and Z. Hu, "Nonreciprocal left handed coplanar waveguide over ferrite substrate with only shunt inductive load," *Microwave and Optical Technology Letters*, Vol. 49, 2810–2814, 2007.
41. Karimian, S., M. Abdalla, and Z. Hu, "Tunable metamaterial ferrite stepped impedance resonator (SIR)," *Progress In Electromagnetics Research Symposium Proceedings*, 165–168, Xi'an, China, Mar. 22–26, 2010.
42. Abdalla, M. A. and Z. Hu, "Compact metamaterial coplanar waveguide ferrite tunable resonator," *IET Microwaves, Antennas & Propagation*, Vol. 10, No. 4, 406–412, 2016.
43. Abdalla, M. A. and Z. Hu, "Multi-band functional tunable LH impedance transformer," *Journal of Electromagnetic Wave and Applications*, Vol. 23, 39–47, 2009.
44. Abdalla, M. A. and Z. Hu, "Compact tunable left handed ferrite transformer," *International Journal of Infrared and Millimeter Waves*, Vol. 30, No. 8, 813–825, 2009.
45. Abdalla, M. and Z. Hu, "Ferrite tunable metamaterial phase shifter," *2010 IEEE AP-S International Antenna and Propagation Symposium Digest*, 1–4, Toronto, Cananda, 2010.
46. Ueda, T., K. Ninomiya, K. Yoshida, and T. Itoh, "Design of dispersion-free phase-shifting non-reciprocity in composite right/left handed metamaterials," *2016 IEEE MTT-S Int. Microwave Symposium (IMS)*, 1–4, 2016.
47. Kodera, T. and C. Caloz, "Integrated leaky-wave antenna-duplexer/diplexer using CRLH uniform ferrite-loaded open waveguide," *IEEE Transactions on Antennas and Propagation*, Vol. 58, No. 8, 2508–2514, 2010.
48. Kodera, T., D. L. Sounas, and C. Caloz, "Tunable magnet-less non-reciprocal metamaterial (MNM) and its application to an isolator," *2012 Asia-Pacific Microwave Conference Proceedings (APMC)*, 73–75, 2012.

49. Abdalla, M. and Z. Hu, "Compact novel CPW ferrite coupled line circulator with left-handed power divider/combiner," *2011 European Microwave Week, EuMW 2011*, 794–797, Manchester, UK, Oct. 9–14, 2011.
50. Sajin, G., S. Simion, F. Craciunoiu, A.-C. Bunea, A. Dinescu, and A. A. Muller, "Ferrite supported steerable antenna on metamaterial CRLH transmission line," *40th European Microwave Conference (EuMC)*, 449–452, 2010.
51. Abdalla, M. and Z. Hu, "Compact and tunable metamaterial antenna for multi-band wireless communication applications," *2011 IEEE AP-S International Antennas and Propagation Symposium Digest*, 2951–2953, Spokane, USA, Jul. 2011.
52. Porokhnyuk, A., T. Ueda, Y. Kado, and T. Itoh, "Design of nonreciprocal CRLH metamaterial for non-squinting leaky-wave antenna," *2013 IEEE MTT-S International Microwave Symposium Digest (IMS)*, 1–3, 2013.
53. Kodera, T., D. L. Sounas, and C. Caloz, "Nonreciprocal magnetless CRLH leaky-wave antenna based on a ring metamaterial structure," *IEEE Antennas and Wireless Propagation Letters*, Vol. 10, 1551–1554, 2011.
54. Sajin, G., I. A. Mocanu, F. Craciunoiu, and M. Carp, "MM-wave left-handed transmission line antenna on anisotropic substrate," *43rd European Microwave Conference (EuMC)*, 668–671, 2013.
55. Tsutsumi, M. and K. Okubo, "Effect of stubs on ferrite microstrip line magnetized to wave propagation," *APMC 2009, Asia Pacific Microwave Conference*, 1234–1237, 2009.
56. Tsutsumi, M. and K. Okubo, "On the left handed ferrite coupled line," *EMTS Int. URSI Electromagnetic Theory Symposium Digest*, 1–3, Ottawa, Canada, 2007.
57. Abdalla, M. A. and Z. Hu, "Compact tunable single and dual mode ferrite left-handed coplanar waveguide coupled line couplers," *IET Microwaves, Antennas & Propagation*, Vol. 3, No. 4, 695–702, 2009.
58. Abdalla, M. A. and Z. Hu, "Composite right/left-handed coplanar waveguide ferrite forward coupled-line coupler," *IET Microwaves, Antennas & Propagation*, Vol. 9, No. 10, 1104–1111, 2015.
59. Abdalla, M. A. and Z. Hu, "Reconfigurable/tunable dual band/dual mode ferrite composite right/left-handed CPW coupled-line coupler," *Journal of Instrumentation*, Vol. 12, No. 9, P09009, 2017.
60. Abdalla, M. A. and Z. Hu, "Tunable characteristics of ferrite composite right/left handed coplanar waveguide coupled line coupler — Measurement and experimental verification," *AEU-International Journal of Electronics and Communications*, Vol. 96, 113–121, 2018.
61. Nguyen, H. V. and C. Caloz, "Generalized coupled mode approach of metamaterial CLCs: Coupling theory, phenomenological explanation, and experimental demonstration," *IEEE Transactions on Microwave Theory and Techniques*, Vol. 55, 1029–1039, May 2007.
62. Pozar, D. M., *Microwave Engineering*, John Wiey & Sons, New York, 1998.
63. Greenhouse, H. M., "Design of planar rectangular microelectronic inductors," *IEEE Transactions on Parts, Hybrids and Packaging*, Vol. 10, 101–109, Jun. 1974.
64. Gupta, K. C., R. Garg, I. Bahl, and P. Bahartia, *Microstrip Lines and Slotlines*, 2nd Edition, Artech House, London, 1996.
65. Aharni, A., "Demagnetizing factor for rectangular ferromagnetic prisms," *Appl. Phys. J.*, Vol. 83, 3432–3434, Mar. 1998.